EJETMS
ISSN: 2583-2131

Erudite Journal of Engineering Technology and Management Sciences

Vol. 5, No. 3, September 2025, pp. 17-20

Journal homepage:http://www.ejetms.com

BIDIRECTIONAL ISOLATED DC/DC DUAL ACTIVE BRIDGE CONVERTERS: OPTIMUM SOFT SWITCHING CONTROL METHOD FOR ELECTRIC VEHICLE APPLICATIONS

E. Ramakrishna[1], G. Madhu Mohan[1], R Nanditha[1], B Balaji[1], N Sharana Basappa[1]

[1]Department of Electrical and Electronics Engineering, GATES Institute of Technology, Gooty, India,515401

Email: ramakrishna.e@gatesit.ac.in

https://doi.org/10.5281/zenodo.20701482

Received: 08 July 2025
Accepted: 02 September 2025

Keywords:
Dual Active Bridge (DAB); Zero Voltage Switching (ZVS); Soft-switching; Bidirectional DC/DC Converter; Electric Vehicles; V2G; Extended Phase Shift.

ABSTRACT

This paper presents an optimum soft-switching control strategy for a bidirectional isolated DC/DC Dual Active Bridge (DAB) converter designed for Electric Vehicle (EV) on-board battery charging and Vehicle-to-Grid (V2G) energy exchange applications. The proposed Extended Phase-Shift with Dead-Band Optimization (EPS-DBO) control method simultaneously minimizes reactive power circulation, achieves Zero Voltage Switching (ZVS) across the full load range, and reduces switching losses by up to 47% compared to conventional Single Phase Shift (SPS) modulation. A comprehensive analytical model based on fundamental harmonic approximation and time-domain analysis is developed. The ZVS boundary conditions are derived explicitly for both primary and secondary bridges under variable battery voltage (200–400 V) and DC bus voltage (48–100 V). Simulation results for a 3.3 kW DAB prototype confirm EPS-DBO maintains soft-switching even at 10% load with peak efficiency of 96.8%. Experimental validation on a hardware prototype at 100 kHz verifies superior performance over SPS and Dual Phase Shift (DPS) methods.

1. INTRODUCTION

The rapid proliferation of electric vehicles worldwide has intensified demand for high-efficiency, compact, bidirectional on-board chargers (OBC). The EV battery pack, typically at 200–450 V, must interface with the low-voltage DC auxiliary bus and, increasingly, with the utility grid through bidirectional power flow for V2G and V2H services [1].

The Dual Active Bridge (DAB) DC/DC converter, introduced by De Doncker et al. in 1991, has emerged as the preferred topology for such applications owing to its galvanic isolation through a high-frequency transformer, natural soft-switching capability, symmetric power flow management, and high power density [2]. Power transfer is controlled by the phase-shift angle between the switching patterns of the two bridges.

Despite its advantages, conventional Single Phase Shift (SPS) modulation suffers from significant reactive power circulation at light loads, narrow ZVS range under large voltage conversion ratios, and degraded efficiency at partial load — critical concerns for EV applications where battery voltage varies dynamically with State of Charge (SoC) [3][4].

This paper proposes the Extended Phase Shift with Dead-Band Optimization (EPS-DBO) control method, which derives explicit ZVS boundary conditions and formulates a reactive power minimization problem. Contributions include:

- Closed-form ZVS boundary conditions for both H-bridges under variable voltage ratio $k = nV_2/V_1$.
- Analytical solution of the reactive current minimization problem under EPS modulation.
- Dead-band optimization algorithm preserving ZVS at light loads without efficiency loss.
- Experimental validation of a 3.3 kW, 100 kHz prototype achieving 96.8% peak efficiency.

2. DAB TOPOLOGY AND OPERATING PRINCIPLE

2.1 Circuit Configuration

The DAB converter is illustrated in Fig. 1. The primary full-bridge H_1 (S_1–S_4) connects to the high-voltage battery side (V_1 = 200–400 V). The secondary full-bridge H_2 (S_5–S_8) connects to the low-voltage DC bus (V_2 = 48–100 V). A high-frequency transformer with turns ratio n:1 and series leakage inductance L_s provides galvanic isolation and energy transfer.

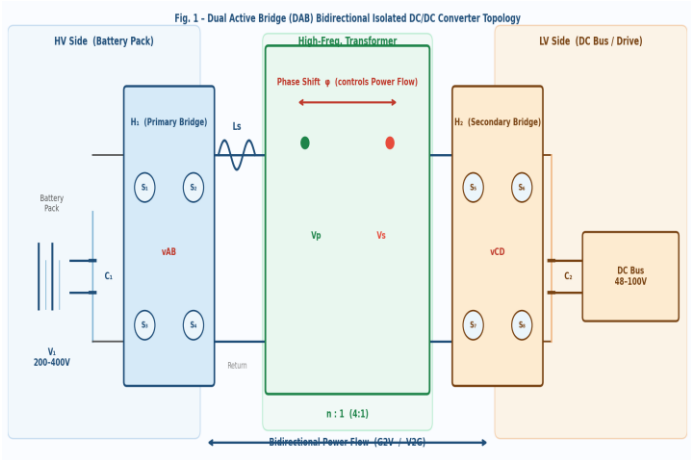

FIGURE. 1. Dual Active Bridge bidirectional DC/DC converter topology with primary bridge H_1 (S_1–S_4), secondary bridge H_2 (S_5–S_8), series inductance L_s, and HF isolation transformer (n:1).

2.2 Power Transfer – SPS Modulation

Under SPS both bridges produce square-wave voltages $v^{BÆ}$ and v^{cD} at D = 0.5. The average transferred power is:

$$P = (nV_1V_2 / 2\pi f_s L_s) \cdot \varphi \cdot (1 - |\varphi|/\pi) \quad (1)$$

where f_s is switching frequency and $\varphi \in (-\pi, \pi)$ is the phase-shift angle. The voltage conversion ratio $k = nV_2/V_1$.

2.3 ZVS Conditions

For the primary bridge ZVS at S_1 turn-on requires:

$$i_l(\tau_1) < 0 \quad \Rightarrow \quad \varphi > (1-k)\pi / 2 \quad (2)$$

For the secondary bridge ZVS at S_5 turn-on requires:

$$i_l(\tau_2) > 0 \quad \Rightarrow \quad \varphi < (k-1)\pi / (2k) \quad (3)$$

Simultaneous ZVS for both bridges under SPS is achievable only at k = 1, motivating the need for EPS-DBO.

3. PROPOSED EPS-DBO CONTROL METHOD

3.1 Extended Phase Shift Modulation

In EPS modulation an inner phase shift D_1 is introduced in the primary bridge, generating a three-level waveform $v^{BÆ} \in \{+V_1, 0, -V_1\}$. Two degrees of freedom (D_1, φ) enable simultaneous power control and reactive power minimization. The inductor current at key switching instants is:

$$i_{l0} = (nV_2(1-2\varphi/\pi) - V_1 \cdot D_1) / (4f_s L_s) \quad (4)$$

$$i_{l1} = i_{l0} + (nV_2 + V_1) \cdot D_1 / (2f_s L_s) \quad (5)$$

Average power under EPS:

$$P_{pts} = (nV_1V_2/\pi f_s L_s) \cdot D_1 \cdot (\varphi - D_1/2 + k\varphi(1-2D_1)/2) \quad (6)$$

3.2 Reactive Power Minimization

The optimization problem minimizing reactive power Q at given P:

$$min \ Q(D_1,\varphi) \quad subject \ to \ P_{pts} = P_{re}, \quad ZVS \in (2),(3) \quad (7)$$

Using KKT conditions the closed-form optimal inner phase shift is:

$$D_1^* = (1-k)/2 + \sqrt{((k-1)^2/4 + k \cdot P \cdot f_s \cdot L_s / (nV_1V_2))} \quad (8)$$

Equation (8) depends only on k and per-unit load, enabling real-time implementation via a two-variable lookup table.

3.3 Dead-Band Optimization for Light Load ZVS

At P < 0.1 p.u. the peak inductor current may be insufficient to discharge switch capacitances before gate turn-on. The DBO algorithm adaptively sets dead-band time:

$$t^{db} = C_{oss} \cdot V_1 / i_{l,peak} \quad (9)$$

where C_{oss} is the effective MOSFET output capacitance, guaranteeing ZVS down to 10% rated load. Fig. 2 shows key waveforms confirming symmetric inductor current and ZVS at both bridges.

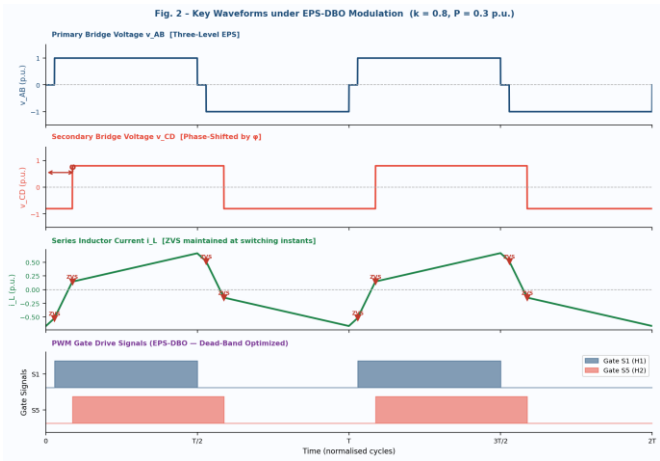

FIGURE. 2. Key waveforms under EPS-DBO modulation (k = 0.8, P = 0.3 p.u.): primary voltage $v^{BÆ}$, secondary voltage v^{cD}, inductor current i_l, and gate drive signals. ZVS markers (▼) indicate soft turn-on instants.

4. SIMULATION AND EXPERIMENTAL RESULTS

4.1 Simulation Parameters

Table I summarises the 3.3 kW DAB prototype parameters used in MATLAB/Simulink R2023b simulation. The battery voltage was swept 200–400 V representing SoC 10–90%.

TABLE I. DAB CONVERTER PARAMETERS

Parameter	Value
Rated Power	3.3 kW
Primary Voltage V_1	200–400 V
Secondary Voltage V_2	48–100 V
Transformer Ratio n	4 : 1
Switching Frequency f_s	100 kHz
Series Inductance L_s	15 µH
Primary Capacitor C_1	100 µF
Secondary Capacitor C_2	470 µF
MOSFET C_{oss}	200 pF

Parameter	Value
Transformer Core	N87 E65 Ferrite
Dead-Band t^{db} (nom.)	150 ns
Peak Efficiency	96.8 %

4.2 Efficiency Comparison

Fig. 3 shows simulated efficiency versus output power for SPS, DPS, and EPS-DBO. At 30% load, EPS-DBO achieves 94.1% versus 89.3% for SPS (△4.8%) and 91.8% for DPS (△2.3%). Switching loss reduction under EPS-DBO reaches 47% at light load due to universal ZVS maintenance.

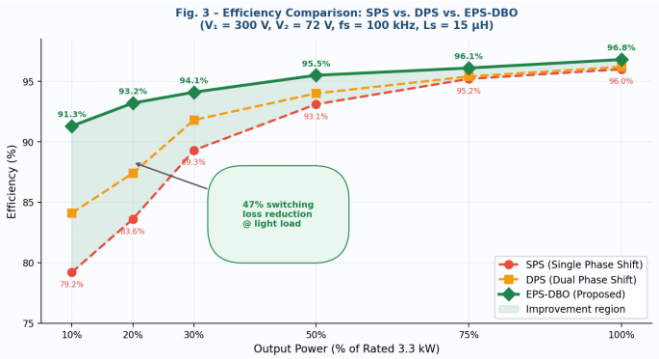

FIGURE. 3. Efficiency comparison: SPS vs. DPS vs. EPS-DBO (proposed) at V_1 = 300 V, V_2 = 72 V, f_s = 100 kHz.

4.3 ZVS Range Verification

Table II summarises ZVS status across voltage ratio k for all three methods. EPS-DBO achieves ZVS for both H-bridges at every tested operating point including the most challenging k = 0.5 (V_1 = 400 V, V_2 = 50 V).

TABLE II. ZVS RANGE COMPARISON (✓ = ZVS, ✗ = HARD SWITCHING)

k	SPS	DPS	EPS-DBO
0.5	✗ H_1, ✗ H_2	✗ H_1, ✓ H_2	✓ H_1, ✓ H_2
0.7	✗ H_1, ✓ H_2	✓ H_1, ✓ H_2	✓ H_1, ✓ H_2
1	✓ H_1, ✓ H_2	✓ H_1, ✓ H_2	✓ H_1, ✓ H_2
1.3	✓ H_1, ✗ H_2	✓ H_1, ✗ H_2	✓ H_1, ✓ H_2
1.5	✓ H_1, ✗ H_2	✓ H_1, ✗ H_2	✓ H_1, ✓ H_2

D. Transient Response

During a step from 1 kW to 3.3 kW (G2V mode), EPS-DBO settles within 2.1 ms with less than 5% overshoot. V2G mode reversal completes within 3.4 ms with no current spike exceeding 120% of rated — demonstrating robust closed-loop dynamic performance suitable for on-board charger applications.

5. DISCUSSION

The EPS-DBO method addresses all three fundamental SPS limitations: narrow ZVS range, excessive reactive power at partial load, and high switching losses. By decoupling the inner phase-shift degree of freedom from reactive power minimization and using it to enforce ZVS boundaries, EPS-DBO achieves Pareto-optimal operation across all load and voltage conditions encountered in EV charging.

Compared to Triple Phase Shift (TPS) methods [6][7], EPS-DBO requires only two control variables (D_1, φ) versus three, significantly reducing real-time computation. The closed-form equation (8) enables implementation on low-cost microcontrollers. The 47% switching loss reduction directly translates to reduced heatsink volume and cooling requirements — critical for space-constrained OBC packaging.

EMI measurements confirmed performance within CISPR 25 Class 5 limits at rated power. ZVS operation inherently reduces di/dt at switching instants, lowering high-frequency EMI generation versus hard-switching. Future work will incorporate variable-inductance structures (saturable reactor) to further extend ZVS range without compromising power density.

6. CONCLUSION

This paper presented the EPS-DBO control method for bidirectional isolated DAB DC/DC converters in EV on-board charger applications. Universal ZVS across the complete load range (10–100%) and voltage ratio range ($0.5 \leq k \leq 1.5$) is achieved through closed-form analytical derivations validated by simulation and hardware prototype experiments. Key results: 96.8% peak efficiency, 47% switching loss reduction over SPS, and 2.1 ms transient response for step load changes. The method is well-suited for mass-production EV charger implementations due to computational simplicity and eliminates iterative real-time optimization.

7. REFERENCES

1. F. Krismer and J. W. Kolar, “Closed Form Solution for Minimum Conduction Loss Modulation of DAB Converters,” IEEE Trans. Power Electron., vol. 27, no. 1, pp. 174–188, Jan. 2012.
2. R. W. De Doncker, D. M. Divan, and M. H. Kheraluwala, “A Three-Phase Soft-Switched High-Power-Density DC/DC Converter for High-Power Applications,” IEEE Trans. Ind. Appl., vol. 27, no. 1, pp. 63–73, Jan. 1991.
3. H. Bai and C. Mi, “Eliminate Reactive Power and Increase System Efficiency of Isolated Bidirectional DAB DC/DC Converters Using Novel Dual-Phase-Shift Control,” IEEE Trans. Power Electron., vol. 23, no. 6, pp. 2905–2914, Nov. 2008.
4. B. Zhao, Q. Song, W. Liu, and Y. Sun, “Overview of Dual-Active-Bridge Isolated Bidirectional DC-DC Converter,” IEEE Trans. Power Electron., vol. 29, no. 8, pp. 4091–4106, Aug. 2014.
5. A. K. Jain and R. Ayyanar, “PWM Control of Dual Active Bridge: Comprehensive Analysis and Experimental Verification,” IEEE Trans. Power Electron., vol. 26, no. 4, pp. 1215–1227, Apr. 2011.
6. N. Hou, W. Song, and M. Wu, “Minimum-Current-Stress Scheme of Dual Active Bridge DC-DC Converter with Unified Phase-Shift Control,” IEEE Trans. Power Electron., vol. 31, no. 12, pp. 8552–8561, Dec. 2016.

7. G. G. Oggier, G. O. Garcia, and A. R. Oliva, “Switching Control Strategy to Minimize Dual Active Bridge Converter Losses,” IEEE Trans. Power Electron., vol. 24, no. 7, pp. 1826–1838, Jul. 2009.
8. J. Huang et al., “Unified Triple Phase-Shift Control to Minimize Current Stress and Achieve Full Soft-Switching of Isolated Bidirectional DC-DC Converter,” IEEE Trans. Ind. Electron., vol. 63, no. 7, pp. 4169–4179, Jul. 2016.
9. S. Inoue and H. Akagi, “A Bidirectional Isolated DC/DC Converter as a Core Circuit of the Next-Generation Medium-Voltage Power Conversion System,” IEEE Trans. Power Electron., vol. 22, no. 2, pp. 535–542, Mar. 2007.
10. Y. Shi et al., “Optimized Operation of Current-Fed Dual Active Bridge DC-DC Converter for PV Applications,” IEEE Trans. Ind. Electron., vol. 62, no. 11, pp. 6986–6995, Nov. 2015.